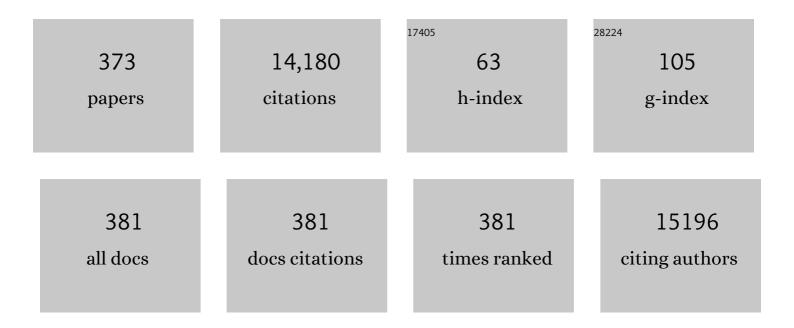
Kazuhito Tsukagoshi

List of Publications by Year in descending order

Source: https://exaly.com/author-pdf/2255611/publications.pdf Version: 2024-02-01



#	Article	lF	CITATIONS
1	C ₆₀ nanowire two-state resistance switching: fabrication and electrical characterizations. Japanese Journal of Applied Physics, 2022, 61, SD0804.	0.8	3
2	Principal Component Analysis of Surface-Enhanced Raman Scattering Spectra Revealing Isomer-Dependent Electron Transport in Spiropyran Molecular Junctions: Implications for Nanoscale Molecular Electronics. ACS Omega, 2022, 7, 5578-5583.	1.6	15
3	Non-invasive digital etching of van der Waals semiconductors. Nature Communications, 2022, 13, 1844.	5.8	8
4	Operando hard X-ray photoelectron spectroscopy study of buried interface chemistry of Au/InO1.16C0.04/Al2O3/p <mml:math <br="" display="inline" xmlns:mml="http://www.w3.org/1998/Math/MathML">id="d1e383" altimg="si20.svg"><mml:msup><mml:mrow /><mml:mrow><mml:mo>+</mml:mo></mml:mrow></mml:mrow </mml:msup></mml:math> -Si stacks. Applied Surface Science, 2022, 593, 153272.	3.1	1
5	Fullerene Nanostructure-Coated Channels Activated by Electron Beam Lithography for Resistance Switching. ACS Applied Nano Materials, 2022, 5, 6430-6437.	2.4	3
6	Fullerene C ₇₀ /porphyrin hybrid nanoarchitectures: single-cocrystal nanoribbons with ambipolar charge transport properties. RSC Advances, 2022, 12, 19548-19553.	1.7	2
7	Nanoarchitectonics of C70 hexagonal nanosheets: Synthesis and charge transport properties. Diamond and Related Materials, 2022, 128, 109217.	1.8	6
8	C ₆₀ -Nanowire Two-State Resistance Switching Based on Fullerene Polymerization/Depolymerization. ACS Applied Nano Materials, 2021, 4, 820-825.	2.4	12
9	Comparison of characteristics of thin-film transistor with In ₂ O ₃ and carbon-doped In ₂ O ₃ channels by atomic layer deposition and post-metallization annealing in O ₃ . Japanese Journal of Applied Physics, 2021, 60, 030903.	0.8	6
10	Influence of adsorbed oxygen concentration on characteristics of carbon-doped indium oxide thin-film transistors under bias stress. Japanese Journal of Applied Physics, 2021, 60, SCCM01.	0.8	3
11	Determination of Chemical Structure of Bis(dithiolato)iron Nanosheet. Chemistry Letters, 2021, 50, 576-579.	0.7	10
12	Tunable Doping of Rhenium and Vanadium into Transition Metal Dichalcogenides for Twoâ€Dimensional Electronics. Advanced Science, 2021, 8, e2004438.	5.6	66
13	Fabrication of WO3 electrochromic devices using electro-exploding wire techniques and spray coating. Solar Energy Materials and Solar Cells, 2021, 223, 110960.	3.0	45
14	Twoâ€Dimensional Bis(dithiolene)iron(II) Selfâ€Powered UV Photodetectors with Ultrahigh Air Stability. Advanced Science, 2021, 8, 2100564.	5.6	19
15	Water Splitting Induced by Visible Light at a Copperâ€Based Singleâ€Molecule Junction. Small, 2021, 17, e2008109.	5.2	3
16	Water Splitting: Water Splitting Induced by Visible Light at a Copperâ€Based Singleâ€Molecule Junction (Small 28/2021). Small, 2021, 17, 2170143.	5.2	0
17	C ₆₀ -Nanowire Two-State Resistance Switching. Journal of Japan Institute of Electronics Packaging, 2021, 24, 401-409.	0.0	0
18	Stable Resistance Switching in Lu ₃ N@C ₈₀ Nanowires Promoted by the Endohedral Effect: Implications for Single-Fullerene Motion Resistance Switching. ACS Applied Nano Materials, 2021, 4, 7935-7942.	2.4	7

#	Article	IF	CITATIONS
19	Splitting charge injection for ultrahigh on/off ratio in a floating-metal-gated planar organic ferroelectric memory. Materials Today Energy, 2021, 21, 100711.	2.5	6
20	Mixed-Salt Enhanced Chemical Vapor Deposition of Two-Dimensional Transition Metal Dichalcogenides. Chemistry of Materials, 2021, 33, 7301-7308.	3.2	22
21	(Invited) Study of HfO ₂ -Based High-k Gate Insulators for GaN Power Device. ECS Transactions, 2021, 104, 113-120.	0.3	2
22	Importance of Annealing Step on Dielectric Constant of ZrO2 Layer of MIM Capacitors with Al2O3/ZrO2 and ZrO2/Al2O3 Stack Structures. ECS Transactions, 2021, 104, 121-128.	0.3	1
23	Visualizing band alignment across 2D/3D perovskite heterointerfaces of solar cells with light-modulated scanning tunneling microscopy. Nano Energy, 2021, 89, 106362.	8.2	13
24	Surface-Enhanced Raman Scattering Stimulated by Strong Metal–Molecule Interactions in a C ₆₀ Single-Molecule Junction. ACS Applied Materials & Interfaces, 2021, 13, 51602-51607.	4.0	9
25	Solution-processed organic single-crystalline semiconductors with a fence-like shape <i>via</i> ultrasound concussion. Journal of Materials Chemistry C, 2020, 8, 2589-2593.	2.7	2
26	One-Dimensional Fullerene/Porphyrin Cocrystals: Near-Infrared Light Sensing through Component Interactions. ACS Applied Materials & Interfaces, 2020, 12, 2878-2883.	4.0	21
27	Unravelling the origin of the photocarrier dynamics of fullerene-derivative passivation of SnO ₂ electron transporters in perovskite solar cells. Journal of Materials Chemistry A, 2020, 8, 23607-23616.	5.2	30
28	Facile and Reversible Carrier-Type Manipulation of Layered MoTe ₂ Toward Long-Term Stable Electronics. ACS Applied Materials & Interfaces, 2020, 12, 42918-42924.	4.0	4
29	Quantum-assisted photoelectric gain effects in perovskite solar cells. NPG Asia Materials, 2020, 12, .	3.8	12
30	Ab-initio investigation of preferential triangular self-formation of oxide heterostructures of monolayer \$\$hbox {WSe}_{2}\$\$. Scientific Reports, 2020, 10, 21737.	1.6	1
31	On/Off Boundary of Photocatalytic Activity between Single- and Bilayer MoS ₂ . ACS Nano, 2020, 14, 6663-6672.	7.3	29
32	Solution-processed organometallic quasi-two-dimensional nanosheets as a hole buffer layer for organic light-emitting devices. Nanoscale, 2020, 12, 6983-6990.	2.8	14
33	Feedback Electromigration Assisted by Alternative Voltage Operation for the Fabrication of Facet-Edge Nanogap Electrodes. ACS Applied Nano Materials, 2020, 3, 4077-4083.	2.4	11
34	Tolerance to Stretching in Thiol-Terminated Single-Molecule Junctions Characterized by Surface-Enhanced Raman Scattering. Journal of Physical Chemistry Letters, 2020, 11, 6712-6717.	2.1	15
35	Solution processed In-Si-O thin film transistors on hydrophilic and hydrophobic substrates. Thin Solid Films, 2020, 698, 137860.	0.8	5
36	Measurement of the Low-Energy Electron Inelastic Mean Free Path in Monolayer Graphene. Physical Review Applied, 2020, 13, .	1.5	10

#	Article	IF	CITATIONS
37	UV degradation mechanism of TiO2-based perovskite solar cells studied by pump-probe spectroscopy. , 2020, , .		7
38	Wafer-scale and deterministic patterned growth of monolayer MoS ₂ <i>via</i> vapor–liquid–solid method. Nanoscale, 2019, 11, 16122-16129.	2.8	76
39	Investigation of Ag and Cu Filament Formation Inside the Metal Sulfide Layer of an Atomic Switch Based on Point-Contact Spectroscopy. ACS Applied Materials & Interfaces, 2019, 11, 27178-27182.	4.0	9
40	Suppression of threshold voltage shift on In-Si-O-C Thin-Film Transistor with an Al2O3 Passivation Layer under Negative and Positive Gate-Bias Stress. , 2019, , .		0
41	Observation of Plasmon Energy Gain for Emitted Secondary Electron in Vacuo. Journal of Physical Chemistry Letters, 2019, 10, 5770-5775.	2.1	8
42	Tunable Chemical Coupling in Two-Dimensional van der Waals Electrostatic Heterostructures. ACS Nano, 2019, 13, 11214-11223.	7.3	13
43	Si-incorporated amorphous indium oxide thin-film transistors. Japanese Journal of Applied Physics, 2019, 58, 090506.	0.8	16
44	Origin of Extended UV Stability of 2D Atomic Layer Titania-Based Perovskite Solar Cells Unveiled by Ultrafast Spectroscopy. ACS Applied Materials & Interfaces, 2019, 11, 21473-21480.	4.0	11
45	Effect of Bias Voltage on a Single-Molecule Junction Investigated by Surface-Enhanced Raman Scattering. Journal of Physical Chemistry C, 2019, 123, 15267-15272.	1.5	6
46	Identifying the molecular adsorption site of a single molecule junction through combined Raman and conductance studies. Chemical Science, 2019, 10, 6261-6269.	3.7	32
47	Stretch dependent electronic structure and vibrational energy of the bipyridine single molecule junction. Physical Chemistry Chemical Physics, 2019, 21, 16910-16913.	1.3	7
48	Near-infrared-light-induced decomposition of Rhodamine B triggered by localized surface plasmon at gold square dimers with well-defined separation distance. AIP Advances, 2019, 9, .	0.6	1
49	Silicon-doped indium oxide – a promising amorphous oxide semiconductor material for thin-film transistor fabricated by spin coating method. IOP Conference Series: Materials Science and Engineering, 2019, 625, 012002.	0.3	2
50	Oxygen-Sensitive Layered MoTe ₂ Channels for Environmental Detection. ACS Applied Materials & Interfaces, 2019, 11, 47047-47053.	4.0	13
51	Selective oxidation of the surface layer of bilayer WSe ₂ by laser heating. Japanese Journal of Applied Physics, 2019, 58, 120903.	0.8	6
52	Characteristics of Oxide TFT Using Carbon-Doped Ιn ₂ O ₃ Thin Film Fabricated by Low-Temperature ALD Using Ethylcyclopentadienyl Indium (Ιn-EtCp) and H ₂ O & O ₃ . ECS Transactions, 2019, 92, 3-13.	0.3	17
53	Si-doping effect on solution-processed In-O thin-film transistors. Materials Research Express, 2019, 6, 026410.	0.8	2
54	Reversible and Precisely Controllable p/nâ€Type Doping of MoTe ₂ Transistors through Electrothermal Doping. Advanced Materials, 2018, 30, e1706995.	11.1	68

#	Article	IF	CITATIONS
55	Unveiling the piezoelectric nature of polar α-phase P(VDF-TrFE) at quasi-two-dimensional limit. Scientific Reports, 2018, 8, 532.	1.6	14
56	Carrier polarity engineering in carbon nanotube field-effect transistors by induced charges in polymer insulator. Applied Physics Letters, 2018, 112, 013501.	1.5	12
57	Pronounced photogating effect in atomically thin WSe2 with a self-limiting surface oxide layer. Applied Physics Letters, 2018, 112, .	1.5	38
58	Fullerene/cobalt porphyrin charge-transfer cocrystals: Excellent thermal stability and high mobility. Nano Research, 2018, 11, 1917-1927.	5.8	27
59	Selfâ€Assembly Atomic Stacking Transport Layer of 2D Layered Titania for Perovskite Solar Cells with Extended UV Stability. Advanced Energy Materials, 2018, 8, 1701722.	10.2	46
60	Reliability of Al2O3/In-Si-O-C Thin-Film Transistors with an Al2O3 Passivation Layer under Gate-Bias Stress. ECS Transactions, 2018, 86, 135-145.	0.3	4
61	Thermal robustness evaluation of nonvolatile memory using Pt nanogaps. Applied Physics Express, 2018, 11, 085202.	1.1	3
62	Investigation on solution-processed In-Si-O thin-film transistor via spin-coating method. , 2018, , .		1
63	Solvent-Mediated Shape Engineering of Fullerene (C ₆₀) Polyhedral Microcrystals. Chemistry of Materials, 2018, 30, 7146-7153.	3.2	37
64	Effect of carbon doping on threshold voltage and mobility of In-Si-O thin-film transistors. Journal of Vacuum Science and Technology B:Nanotechnology and Microelectronics, 2018, 36, 061206.	0.6	5
65	Dependence of Stretch Length on Electrical Conductance and Electronic Structure of the Benzenedithiol Single Molecular Junction. E-Journal of Surface Science and Nanotechnology, 2018, 16, 145-149.	0.1	2
66	Layer-by-Layer Oxidation Induced Electronic Properties in Transition-Metal Dichalcogenides. Journal of Physical Chemistry C, 2018, 122, 17001-17007.	1.5	12
67	Photochemical Reaction Using Aminobenzenethiol Single Molecular Junction. E-Journal of Surface Science and Nanotechnology, 2018, 16, 137-141.	0.1	2
68	<i>In situ</i> observation of the formation process for free-standing Au nanowires with a scanning electron microscope. Nanotechnology, 2017, 28, 105707.	1.3	2
69	Amorphous In-Si-O Films Fabricated via Solution Processing. Journal of Electronic Materials, 2017, 46, 3610-3614.	1.0	7
70	Virtual substrate method for nanomaterials characterization. Nature Communications, 2017, 8, 15629.	5.8	25
71	Correlation between active layer thickness and ambient gas stability in IGZO thin-film transistors. Journal Physics D: Applied Physics, 2017, 50, 025102.	1.3	4
72	Controlling the thermoelectric effect by mechanical manipulation of the electron's quantum phase in atomic junctions. Scientific Reports, 2017, 7, 7949.	1.6	12

#	Article	IF	CITATIONS
73	Flexible and Printed Electronics. Japanese Journal of Applied Physics, 2017, 56, 05E001.	0.8	1
74	Radial Interference Contrast in in-situ SEM Observation of Metal Oxide Semiconductor Film Crystallization. Microscopy and Microanalysis, 2017, 23, 1512-1513.	0.2	1
75	Gap width-independent spectra in 4-aminothiophenol surface enhanced Raman scattering stimulated in Au-gap array. Japanese Journal of Applied Physics, 2017, 56, 065202.	0.8	3
76	Self-powered graphene thermistor. Nano Energy, 2016, 26, 586-594.	8.2	27
77	Phase transitions from semiconductive amorphous to conductive polycrystalline in indium silicon oxide thin films. Applied Physics Letters, 2016, 109, .	1.5	13
78	Anomalous behavior of 1/ <i>f</i> noise in graphene near the charge neutrality point. Applied Physics Letters, 2016, 108, .	1.5	11
79	Homogeneous double-layer amorphous Si-doped indium oxide thin-film transistors for control of turn-on voltage. Journal of Applied Physics, 2016, 120, .	1.1	19
80	Carrier Polarity Control in α-MoTe ₂ Schottky Junctions Based on Weak Fermi-Level Pinning. ACS Applied Materials & Interfaces, 2016, 8, 14732-14739.	4.0	72
81	Prospectively of Carbon-Doped Indium-Tungsten-Oxide Channel TFT for Bias Stress Instability. ECS Transactions, 2016, 75, 149-156.	0.3	5
82	Two-dimensional MoTe ₂ materials: From synthesis, identification, and charge transport to electronics applications. Japanese Journal of Applied Physics, 2016, 55, 1102A1.	0.8	20
83	High-performance non-volatile field-effect transistor memories using an amorphous oxide semiconductor and ferroelectric polymer. Journal of Materials Chemistry C, 2016, 4, 7917-7923.	2.7	15
84	Highly stable, extremely high-temperature, nonvolatile memory based on resistance switching in polycrystalline Pt nanogaps. Scientific Reports, 2016, 6, 34961.	1.6	12
85	Hunting for Monolayer Oxide Nanosheets and Their Architectures. Scientific Reports, 2016, 6, 19402.	1.6	23
86	Determination of the number of atoms present in nano contact based on shot noise measurements with highly stable nano-fabricated electrodes. Nanotechnology, 2016, 27, 295203.	1.3	2
87	Self-Limiting Oxides on WSe ₂ as Controlled Surface Acceptors and Low-Resistance Hole Contacts. Nano Letters, 2016, 16, 2720-2727.	4.5	131
88	Improvement of the effective work function and transmittance of thick indium tin oxide/ultrathin ruthenium doped indium oxide bilayers as transparent conductive oxide. Thin Solid Films, 2016, 598, 126-130.	0.8	3
89	Site-Selection in Single-Molecule Junction for Highly Reproducible Molecular Electronics. Journal of the American Chemical Society, 2016, 138, 1294-1300.	6.6	88
90	Charge transport and mobility engineering in two-dimensional transition metal chalcogenide semiconductors. Chemical Society Reviews, 2016, 45, 118-151.	18.7	423

#	Article	IF	CITATIONS
91	Nanocontact Disorder in Nanoelectronics for Modulation of Light and Gas Sensitivities. Scientific Reports, 2015, 5, 13035.	1.6	9
92	Codoping of zinc and tungsten for practical high-performance amorphous indium-based oxide thin film transistors. Journal of Applied Physics, 2015, 118, .	1.1	23
93	Influence of Al2O3 layer insertion on the electrical properties of Ga-In-Zn-O thin-film transistors. Journal of Vacuum Science and Technology A: Vacuum, Surfaces and Films, 2015, 33, .	0.9	6
94	Reducing contact resistance in ferroelectric organic transistors by buffering the semiconductor/dielectric interface. Applied Physics Letters, 2015, 107, .	1.5	21
95	Origin of Noise in Layered MoTe ₂ Transistors and its Possible Use for Environmental Sensors. Advanced Materials, 2015, 27, 6612-6619.	11.1	72
96	Electrostatically Reversible Polarity of Ambipolar α-MoTe ₂ Transistors. ACS Nano, 2015, 9, 5976-5983.	7.3	113
97	Epitaxial CVD growth of high-quality graphene and recent development of 2D heterostructures. , 2015, , .		0
98	Wafer-scale fabrication of transistors using CVD-grown graphene and its application to inverter circuit. Japanese Journal of Applied Physics, 2015, 54, 04DN06.	0.8	6
99	Self-Limiting Layer-by-Layer Oxidation of Atomically Thin WSe ₂ . Nano Letters, 2015, 15, 2067-2073.	4.5	204
100	Dopant selection for control of charge carrier density and mobility in amorphous indium oxide thin-film transistors: Comparison between Si- and W-dopants. Applied Physics Letters, 2015, 106, .	1.5	56
101	Suppression of excess oxygen for environmentally stable amorphous In-Si-O thin-film transistors. Applied Physics Letters, 2015, 106, .	1.5	25
102	Parity effect of bipolar quantum Hall edge transport around graphene antidots. Scientific Reports, 2015, 5, 11723.	1.6	7
103	Double resonance Raman modes in monolayer and few-layer <mml:math xmlns:mml="http://www.w3.org/1998/Math/MathML"><mml:msub><mml:mi mathvariant="normal">MoTe<mml:mn>2</mml:mn></mml:mi </mml:msub>. Physical Review B. 2015, 91</mml:math 	1.1	99
104	Edge mixing dynamics in graphene p–n junctions in the quantum Hall regime. Nature Communications, 2015, 6, 8066.	5.8	28
105	Reduction of the interfacial trap density of indium-oxide thin film transistors by incorporation of hafnium and annealing process. AIP Advances, 2015, 5, .	0.6	16
106	Carrier Injection and Scattering in Atomically Thin Chalcogenides. Journal of the Physical Society of Japan, 2015, 84, 121011.	0.7	7
107	Solution-assembled nanowires for high performance flexible and transparent solar-blind photodetectors. Journal of Materials Chemistry C, 2015, 3, 596-600.	2.7	45
108	Impact of Carbon-Doped ï¼ ©n-Si-O Channel for Future TFT. ECS Meeting Abstracts, 2015, , .	0.0	0

#	Article	IF	CITATIONS
109	Influence of Al ₂ O ₃ Gate Dielectric on Transistor Properties for IGZO Thin Film Transistor. ECS Transactions, 2014, 61, 345-351.	0.3	2
110	Stable amorphous In2O3-based thin-film transistors by incorporating SiO2 to suppress oxygen vacancies. Applied Physics Letters, 2014, 104, .	1.5	83
111	Low-temperature processable amorphous In-W-O thin-film transistors with high mobility and stability. Applied Physics Letters, 2014, 104, 152103.	1.5	79
112	Modulation of effective damping constant using spin Hall effect. Applied Physics Letters, 2014, 104, 092408.	1.5	37
113	Controllable film densification and interface flatness for high-performance amorphous indium oxide based thin film transistors. Applied Physics Letters, 2014, 105, .	1.5	9
114	Spin injection and detection in a graphene lateral spin valve using an yttrium-oxide tunneling barrier. Applied Physics Express, 2014, 7, 085101.	1.1	6
115	Self-formed copper oxide contact interlayer for high-performance oxide thin film transistors. Applied Physics Letters, 2014, 105, .	1.5	13
116	Ambipolar MoTe ₂ Transistors and Their Applications in Logic Circuits. Advanced Materials, 2014, 26, 3263-3269.	11.1	388
117	Thickness Scaling Effect on Interfacial Barrier and Electrical Contact to Two-Dimensional MoS ₂ Layers. ACS Nano, 2014, 8, 12836-12842.	7.3	149
118	Large [6,6]-phenyl C61 butyric acid methyl (PCBM) hexagonal crystals grown by solvent-vapor annealing. Materials Chemistry and Physics, 2014, 145, 327-333.	2.0	13
119	Control of molecular orientation and morphology in organic bilayer solar cells: Copper phthalocyanine on gold nanodots. Thin Solid Films, 2014, 562, 467-470.	0.8	9
120	Patterning technology for solution-processed organic crystal field-effect transistors. Science and Technology of Advanced Materials, 2014, 15, 024203.	2.8	39
121	Highly stable Au atomic contacts covered with benzenedithiol under ambient conditions. Physical Chemistry Chemical Physics, 2014, 16, 15662.	1.3	10
122	Barrier inhomogeneities at vertically stacked graphene-based heterostructures. Nanoscale, 2014, 6, 795-799.	2.8	64
123	Electrostatically Reversible Polarity of Dual-Gated Graphene Transistors. IEEE Nanotechnology Magazine, 2014, 13, 1039-1043.	1.1	14
124	Semiconducting properties of bilayer graphene modulated by an electric field for next-generation atomic-film electronics. Journal Physics D: Applied Physics, 2014, 47, 094003.	1.3	7
125	Strong Enhancement of Raman Scattering from a Bulk-Inactive Vibrational Mode in Few-Layer MoTe ₂ . ACS Nano, 2014, 8, 3895-3903.	7.3	275
126	Structure and transport properties of the interface between CVD-grown graphene domains. Nanoscale, 2014, 6, 7288.	2.8	52

#	Article	IF	CITATIONS
127	Strainâ€Tunable Superconducting Fieldâ€Effect Transistor with an Organic Stronglyâ€Correlated Electron System. Advanced Materials, 2014, 26, 3490-3495.	11.1	29
128	Boost Up Carrier Mobility for Ferroelectric Organic Transistor Memory via Buffering Interfacial Polarization Fluctuation. Scientific Reports, 2014, 4, 7227.	1.6	67
129	Metal atomic contacts under defined environmental conditions. Transactions of the Materials Research Society of Japan, 2014, 39, 225-229.	0.2	Ο
130	Thickness-Dependent Interfacial Coulomb Scattering in Atomically Thin Field-Effect Transistors. Nano Letters, 2013, 13, 3546-3552.	4.5	285
131	Rational design of a high performance all solid state flexible micro-supercapacitor on paper. RSC Advances, 2013, 3, 15827.	1.7	45
132	Lowâ€Cost Fully Transparent Ultraviolet Photodetectors Based on Electrospun ZnO‧nO ₂ Heterojunction Nanofibers. Advanced Materials, 2013, 25, 4625-4630.	11.1	275
133	High-performance top-gated monolayer SnS2 field-effect transistors and their integrated logic circuits. Nanoscale, 2013, 5, 9666.	2.8	269
134	On Practical Charge Injection at the Metal/Organic Semiconductor Interface. Scientific Reports, 2013, 3, 1026.	1.6	71
135	Suppression of thermally activated carrier transport in atomically thin MoS2 on crystalline hexagonal boron nitride substrates. Nanoscale, 2013, 5, 9572.	2.8	69
136	Epitaxial Growth and Electronic Properties of Large Hexagonal Graphene Domains on Cu(111) Thin Film. Applied Physics Express, 2013, 6, 075101.	1.1	83
137	Self-Aligned Formation of Sub 1 nm Gaps Utilizing Electromigration during Metal Deposition. ACS Applied Materials & amp; Interfaces, 2013, 5, 12869-12875.	4.0	23
138	Self-assembly of semiconductor/insulator interfaces in one-step spin-coating: a versatile approach for organic field-effect transistors. Physical Chemistry Chemical Physics, 2013, 15, 7917.	1.3	59
139	Realization of graphene field-effect transistor with high-κ HCa2Nb3O10 nanoflake as top-gate dielectric. Applied Physics Letters, 2013, 103, .	1.5	12
140	Understanding Thickness-Dependent Charge Transport in Pentacene Transistors by Low-Frequency Noise. IEEE Electron Device Letters, 2013, 34, 1298-1300.	2.2	19
141	Flexible SnO2 hollow nanosphere film based high-performance ultraviolet photodetector. Chemical Communications, 2013, 49, 3739.	2.2	93
142	Structural and charge transport characteristics of graphene layers obtained from CVD thin film and bulk graphite materials. Carbon, 2013, 52, 49-55.	5.4	12
143	In situpurification to eliminate the influence of impurities in solution-processed organic crystals for transistor arrays. Journal of Materials Chemistry C, 2013, 1, 1352-1358.	2.7	37
144	Conduction Tuning of Graphene Based on Defect-Induced Localization. ACS Nano, 2013, 7, 5694-5700.	7.3	78

#	Article	IF	CITATIONS
145	Contact Thickness Effects in Bottom-Contact Coplanar Organic Field-Effect Transistors. IEEE Electron Device Letters, 2013, 34, 535-537.	2.2	13
146	How small the contacts could be optimal for nanoscale organic transistors?. Organic Electronics, 2013, 14, 1797-1804.	1.4	16
147	Effects of dopants in InOx-based amorphous oxide semiconductors for thin-film transistor applications. Applied Physics Letters, 2013, 103, .	1.5	103
148	Joule's law for organic transistors exploration: Case of contact resistance. Journal of Applied Physics, 2013, 113, 064507.	1.1	19
149	Thin-film transistors fabricated by low-temperature process based on Ga- and Zn-free amorphous oxide semiconductor. Applied Physics Letters, 2013, 102, .	1.5	59
150	Current onâ€off operation of graphene transistor with dual gates and He ion irradiated channel. Physica Status Solidi C: Current Topics in Solid State Physics, 2013, 10, 1608-1611.	0.8	5
151	Flexible field-effect transistor arrays with patterned solution-processed organic crystals. AIP Advances, 2013, 3, .	0.6	19
152	Surface Selectively Deposited Organic Single-crystal Transistor Arrays with High Device Performance. Molecular Crystals and Liquid Crystals, 2012, 566, 13-17.	0.4	4
153	Metal-diffusion-induced ITO nanoparticles at the organic/ITO interface. Journal Physics D: Applied Physics, 2012, 45, 165104.	1.3	3
154	Charge trapping at organic/self-assembly molecule interfaces studied by electrical switching behaviour in a crosspoint structure. Journal Physics D: Applied Physics, 2012, 45, 025304.	1.3	1
155	Control of neural signal propagation in neuron by three terminal electrodes method. Electronics Letters, 2012, 48, 1093-1095.	0.5	Ο
156	Temperature dependence of frequency response characteristics in organic field-effect transistors. Applied Physics Letters, 2012, 100, 183308.	1.5	10
157	Highly enhanced charge injection in thienoacene-based organic field-effect transistors with chemically doped contact. Applied Physics Letters, 2012, 100, .	1.5	130
158	Reduction of charge injection barrier by 1-nm contact oxide interlayer in organic field effect transistors. Applied Physics Letters, 2012, 100, .	1.5	37
159	Role of atomic terraces and steps in the electron transport properties of epitaxial graphene grown on SiC. AIP Advances, 2012, 2, .	0.6	21
160	Gate-Controlled P–I–N Junction Switching Device with Graphene Nanoribbon. Applied Physics Express, 2012, 5, 015101.	1.1	17
161	Single-Crystalline Nanogap Electrodes: Enhancing the Nanowire-Breakdown Process with a Gaseous Environment. ACS Applied Materials & Interfaces, 2012, 4, 5542-5546.	4.0	14
162	Direct formation of organic semiconducting single crystals by solvent vapor annealing on a polymer base film. Journal of Materials Chemistry, 2012, 22, 8462.	6.7	55

#	Article	IF	CITATIONS
163	Concerted Chemical-Mechanical Reaction in Catalyzed Growth of Confined Graphene Layers into Hexagonal Disks. Journal of Physical Chemistry C, 2012, 116, 9106-9113.	1.5	1
164	Evaluation of Spin Hall Angle and Spin Diffusion Length by Using Spin Current-Induced Ferromagnetic Resonance. Applied Physics Express, 2012, 5, 073002.	1.1	138
165	Origin of the relatively low transport mobility of graphene grown through chemical vapor deposition. Scientific Reports, 2012, 2, 337.	1.6	159
166	Controllable gallium melt-assisted interfacial graphene growth on silicon carbide. Diamond and Related Materials, 2012, 24, 34-38.	1.8	7
167	Tunable contact resistance in double-gate organic field-effect transistors. Organic Electronics, 2012, 13, 1583-1588.	1.4	18
168	Observation of Tunneling Current in Semiconducting Graphenep–nJunctions. Journal of the Physical Society of Japan, 2012, 81, 014708.	0.7	8
169	Controlling the crystal formation in solution-process for organic field-effect transistors with high-performance. Organic Electronics, 2012, 13, 2975-2984.	1.4	17
170	Quantitative Raman Spectrum and Reliable Thickness Identification for Atomic Layers on Insulating Substrates. ACS Nano, 2012, 6, 7381-7388.	7.3	322
171	Solution-processed, Self-organized Organic Single Crystal Arrays with Controlled Crystal Orientation. Scientific Reports, 2012, 2, 393.	1.6	87
172	Liquid phase growth of graphene on silicon carbide. Carbon, 2012, 50, 5076-5084.	5.4	18
173	High-performance organic field-effect transistors based on dihexyl-substituted dibenzo[d,d′]thieno[3,2-b;4,5-b′]dithiophene. Journal of Materials Chemistry, 2012, 22, 7715.	6.7	37
174	Enhanced current-rectification in bilayer graphene with an electrically tuned sloped bandgap. Nanoscale, 2012, 4, 7842.	2.8	13
175	Unipolar transport in bilayer graphene controlled by multiple <i>p-n</i> interfaces. Applied Physics Letters, 2012, 100, .	1.5	12
176	Electrostatically-reversible polarity of dual-gated graphene transistors with He ion irradiated channel: Toward reconfigurable CMOS applications. , 2012, , .		16
177	Optimal Structure for Highâ€Performance and Lowâ€Contactâ€Resistance Organic Fieldâ€Effect Transistors Using Contactâ€Doped Coplanar and Pseudoâ€Staggered Device Architectures. Advanced Functional Materials, 2012, 22, 4577-4583.	7.8	57
178	Large plate-like organic crystals from direct spin-coating for solution-processed field-effect transistor arrays with high uniformity. Organic Electronics, 2012, 13, 264-272.	1.4	69
179	Solution-processed organic crystals for field-effect transistor arrays with smooth semiconductor/dielectric interface on paper substrates. Organic Électronics, 2012, 13, 815-819.	1.4	65
180	Forming semiconductor/dielectric double layers by one-step spin-coating for enhancing the performance of organic field-effect transistors. Organic Electronics, 2012, 13, 1146-1151.	1.4	39

#	Article	IF	CITATIONS
181	Controlled Selfâ€Assembly of Organic Semiconductors for Solutionâ€Based Fabrication of Organic Fieldâ€Effect Transistors. Advanced Materials, 2012, 24, 299-306.	11.1	104
182	Bottom-Contact Pentacene Thin-Film Transistors on Silicon Nitride. IEEE Electron Device Letters, 2011, 32, 1305-1307.	2.2	8
183	Analysis of low-frequency noise in organic field-effect transistors combining static and noise data. , 2011, , .		Ο
184	Enhanced Logic Performance with Semiconducting Bilayer Graphene Channels. ACS Nano, 2011, 5, 500-506.	7.3	40
185	Carrier mobility in organic field-effect transistors. Journal of Applied Physics, 2011, 110, 104513.	1.1	43
186	Patterning solution-processed organic single-crystal transistors with high device performance. AIP Advances, 2011, 1, .	0.6	45
187	Power transfer-length method for full biasing contact resistance evaluation of organic field-effect transistors. Organic Electronics, 2011, 12, 2019-2024.	1.4	16
188	Unipolar resistive switching in high-resistivity Pr0.7Ca0.3MnO3 junctions. Applied Physics A: Materials Science and Processing, 2011, 103, 21-26.	1.1	11
189	Origin of low-frequency noise in pentacene field-effect transistors. Solid-State Electronics, 2011, 61, 106-110.	0.8	45
190	Complementary‣ike Graphene Logic Gates Controlled by Electrostatic Doping. Small, 2011, 7, 1552-1556.	5.2	45
191	Solutionâ€Processable Organic Single Crystals with Bandlike Transport in Fieldâ€Effect Transistors. Advanced Materials, 2011, 23, 523-526.	11.1	348
192	Control of device parameters by active layer thickness in organic field-effect transistors. Applied Physics Letters, 2011, 98, .	1.5	28
193	Introducing Nonuniform Strain to Graphene Using Dielectric Nanopillars. Applied Physics Express, 2011, 4, 075102.	1.1	101
194	Electric-field-induced Mott transition in an organic molecular crystal. Physical Review B, 2011, 84, .	1.1	28
195	Diagnosis of low-frequency noise sources in contact resistance of staggered organic transistors. Applied Physics Letters, 2011, 98, 033505.	1.5	9
196	Modeling of static electrical properties in organic field-effect transistors. Journal of Applied Physics, 2011, 110, 014510.	1.1	21
197	Effect of air exposure on metal/organic interface in organic field-effect transistors. Applied Physics Letters, 2011, 98, 243301.	1.5	22
198	Volatile/Nonvolatile Dual-Functional Atom Transistor. Applied Physics Express, 2011, 4, 015204.	1.1	42

#	Article	IF	CITATIONS
199	Gate-Voltage Modulation in Graphene. , 2011, , 179-187.		1
200	Effect of current annealing on electronic properties of multilayer graphene. Journal of Physics: Conference Series, 2010, 232, 012015.	0.3	5
201	Inverse spin valve effect in multilayer graphene device. Journal of Physics: Conference Series, 2010, 232, 012002.	0.3	Ο
202	Extraction of low-frequency noise in contact resistance of organic field-effect transistors. Applied Physics Letters, 2010, 97, .	1.5	24
203	All-Solution-Processed Selective Assembly of Flexible Organic Field-Effect Transistor Arrays. Applied Physics Express, 2010, 3, 051601.	1.1	37
204	Present Status and Possibilities of Graphene Electron Transport. Journal of the Vacuum Society of Japan, 2010, 53, 85-93.	0.3	0
205	Dependence of proximity-induced supercurrent on junction length in multilayer-graphene Josephson junctions. Physica C: Superconductivity and Its Applications, 2010, 470, 1477-1480.	0.6	14
206	Fabrication of ultrashort graphene Josephson junctions. Physica C: Superconductivity and Its Applications, 2010, 470, 1492-1495.	0.6	14
207	Siteâ€selective deposition of singleâ€wall carbon nanotubes by patterning selfâ€assembled monolayer for application to thinâ€film transistors. Physica Status Solidi (B): Basic Research, 2010, 247, 2750-2753.	0.7	12
208	Memory Effect in Simple Cu Nanogap Junction. Materials Research Society Symposia Proceedings, 2010, 1250, 1.	0.1	0
209	Determination of the Number of Graphene Layers: Discrete Distribution of the Secondary Electron Intensity Stemming from Individual Graphene Layers. Applied Physics Express, 2010, 3, 095101.	1.1	81
210	All-solution-processed selective assembly of flexible organic field-effect transistor arrays. Proceedings of SPIE, 2010, , .	0.8	1
211	Pulsed Bias Stress in Pentacene Thin Film Transistors and Effect of Contact Material. Japanese Journal of Applied Physics, 2010, 49, 01AB03.	0.8	2
212	Toward sub-20 nm hybrid nanofabrication by combining the molecular ruler method and electron beam lithography. Nanotechnology, 2010, 21, 495304.	1.3	5
213	Resistance modulation of multilayer graphene controlled by the gate electric field. Semiconductor Science and Technology, 2010, 25, 034008.	1.0	30
214	Influence of Disorder on Conductance in Bilayer Graphene under Perpendicular Electric Field. Nano Letters, 2010, 10, 3888-3892.	4.5	116
215	Influence of electrode size on resistance switching effect in nanogap junctions. Applied Physics Letters, 2010, 97, 073118.	1.5	25
216	Understanding contact behavior in organic thin film transistors. Applied Physics Letters, 2010, 97, 063307.	1.5	70

#	Article	IF	CITATIONS
217	Direct evaluation of low-field mobility and access resistance in pentacene field-effect transistors. Journal of Applied Physics, 2010, 107, .	1.1	181
218	Low Operating Bias and Matched Inputâ^'Output Characteristics in Graphene Logic Inverters. Nano Letters, 2010, 10, 2357-2362.	4.5	105
219	Transition-Voltage Method for Estimating Contact Resistance in Organic Thin-Film Transistors. IEEE Electron Device Letters, 2010, 31, 509-511.	2.2	35
220	Anisotropic transport in graphene on SiC substrate with periodic nanofacets. Applied Physics Letters, 2010, 96, 062111.	1.5	29
221	Fabrication of graphene device and gate-voltage characterization. Tanso, 2010, 2010, 110-115.	0.1	0
222	Contact resistance instability in pentacene thin film transistors induced by ambient gases. Applied Physics Letters, 2009, 94, 083309.	1.5	18
223	Field-Induced Carrier Delocalization in the Strain-Induced Mott Insulating State of an Organic Superconductor. Physical Review Letters, 2009, 103, 116801.	2.9	49
224	Improvement of subthreshold current transport by contact interface modification in p-type organic field-effect transistors. Applied Physics Letters, 2009, 94, .	1.5	164
225	Surface selective deposition of molecular semiconductors for solution-based integration of organic field-effect transistors. Applied Physics Letters, 2009, 94, .	1.5	96
226	Study of Organic Material FETs by Combined Static and Noise Measurements. , 2009, , .		1
227	Thinâ€film transistors fabricated from semiconductorâ€enriched singleâ€wall carbon nanotubes. Physica Status Solidi (B): Basic Research, 2009, 246, 2849-2852.	0.7	3
228	Field effect on organic charge-ordered/Mott insulators. Physica B: Condensed Matter, 2009, 404, 413-415.	1.3	9
229	Simple and Scalable Gel-Based Separation of Metallic and Semiconducting Carbon Nanotubes. Nano Letters, 2009, 9, 1497-1500.	4.5	307
230	Ambipolar-transporting coaxial nanotubes with a tailored molecular graphene–fullerene heterojunction. Proceedings of the National Academy of Sciences of the United States of America, 2009, 106, 21051-21056.	3.3	161
231	Charge Transport Properties of Hexabenzocoronene Nanotubes by Field Effect: Influence of the Oligoether Side Chains on the Mobility. Chemistry Letters, 2009, 38, 888-889.	0.7	17
232	A different type of reentrant behavior in superconductor/thin graphite film/superconductor Josephson junctions. Physica C: Superconductivity and Its Applications, 2008, 468, 797-800.	0.6	6
233	Gate-controlled superconducting proximity effect in ultrathin graphite films. Physica E: Low-Dimensional Systems and Nanostructures, 2008, 40, 1495-1497.	1.3	18

234 Conduction properties of micro-crystals of 2,5-dimethyl-N,N $\hat{a}\in^2$ -dicyanoquinonediimine metal (metal=Ag,) Tj ETQqQQQ 0 rgBT $\frac{1}{5}$ Overlock 2.5 dimethyl-N,N $\hat{a}\in^2$ -dicyanoquinonediimine metal (metal=Ag,) Tj ETQqQQQ 0 rgBT $\frac{1}{5}$ Overlock 2.5 dimethyl-N,N $\hat{a}\in^2$ -dicyanoquinonediimine metal (metal=Ag,) Tj ETQqQQQ 0 rgBT $\frac{1}{5}$ Overlock 2.5 dimethyl-N,N $\hat{a}\in^2$ -dicyanoquinonediimine metal (metal=Ag,) Tj ETQqQQQ 0 rgBT $\frac{1}{5}$ Overlock 2.5 dimethyl-N,N $\hat{a}\in^2$ -dicyanoquinonediimine metal (metal=Ag,) Tj ETQqQQQ 0 rgBT $\frac{1}{5}$ Overlock 2.5 dimethyl-N,N $\hat{a}\in^2$ -dicyanoquinonediimine metal (metal=Ag,) Tj ETQqQQQ 0 rgBT $\frac{1}{5}$ Overlock 2.5 dimethyl-N,N $\hat{a}\in^2$ -dicyanoquinonediimine metal (metal=Ag,) Tj ETQqQQQ 0 rgBT $\frac{1}{5}$ Overlock 2.5 dimethyl-N,N $\hat{a}\in^2$ -dicyanoquinonediimine metal (metal=Ag,) Tj ETQqQQQ 0 rgBT $\frac{1}{5}$ Overlock 2.5 dimethyl-N,N $\hat{a}\in^2$ -dicyanoquinonediimine metal (metal=Ag,) Tj ETQqQQQ 0 rgBT $\frac{1}{5}$ Overlock 2.5 dimethyl-N,N $\hat{a}\in^2$ -dicyanoquinonediimine metal (metal=Ag,) Tj ETQqQQ 0 rgBT $\frac{1}{5}$ Overlock 2.5 dimethyl-N,N $\hat{a}\in^2$ -dicyanoquinonediimine metal (metal=Ag,) Tj ETQqQQ 0 rgBT $\frac{1}{5}$ Overlock 2.5 dimethyl-N,N $\hat{a}\in^2$ -dicyanoquinonediimine metal (metal=Ag,) Tj ETQqQQ 0 rgBT $\frac{1}{5}$ Overlock 2.5 dimethyl-N,N $\hat{a}\in^2$ -dicyanoquinonediimine metal (metal=Ag,) Tj ETQqQ 0 rgBT $\frac{1}{5}$ Overlock 2.5 dimethyl-N,N $\hat{a}\in^2$ -dicyanoquinonediimine metal (metal=Ag,) Tj ETQqQ 0 rgBT $\frac{1}{5}$ Overlock 2.5 dimethyl-N,N $\hat{a}\in^2$ -dicyanoquinonediimine metal (metal=Ag,) Tj ETQqQ 0 rgBT $\frac{1}{5}$

#	ARTICLE	IF	CITATIONS
235	Bias stress instability in pentacene thin film transistors: Contact resistance change and channel threshold voltage shift. Applied Physics Letters, 2008, 92, 063305.	1.5	90
236	Gate control of spin transport in multilayer graphene. Applied Physics Letters, 2008, 92, 212110.	1.5	72
237	Coulomb Blockade Oscillations in Patterned Ultrathin Graphite Films. Japanese Journal of Applied Physics, 2008, 47, 697-699.	0.8	1
238	Charge trapping induced current instability in pentacene thin film transistors: Trapping barrier and effect of surface treatment. Applied Physics Letters, 2008, 93, .	1.5	78
239	Strain-induced superconductor/insulator transition and field effect in a thin single crystal of molecular conductor. Applied Physics Letters, 2008, 92, 243508.	1.5	63
240	Direct observation of the electronic states of single crystalline rubrene under ambient condition by photoelectron yield spectroscopy. Applied Physics Letters, 2008, 93, 173305.	1.5	76
241	Dynamic bias stress current instability caused by charge trapping and detrapping in pentacene thin film transistors. Applied Physics Letters, 2008, 93, .	1.5	13
242	Selective organization of solution-processed organic field-effect transistors. Applied Physics Letters, 2008, 92, .	1.5	74
243	Correlation between grain size and device parameters in pentacene thin film transistors. Applied Physics Letters, 2008, 93, .	1.5	93
244	Observation of gate-controlled superconducting proximity effect in microfabricated thin graphite films. Journal of Physics: Conference Series, 2008, 109, 012031.	0.3	0
245	Superconducting Proximity Effect in Multilayer Graphene. Hyomen Kagaku, 2008, 29, 315-320.	0.0	0
246	āfŠāfŽāfāf¥āf¼āf—電極ā,'用ā"āŸāfŠāfŽā,®āf£āffāf—有機āf^āf©āf³ā,¸ā,¹ā,¿. Journal of the Va	cuumaSoci	etyœf Japan, 2
247	Defect-free two-dimensional-photonic crystal structures on a nonlinear optical polymer patterned by nanoimprint lithography. Journal of Vacuum Science & Technology B, 2007, 25, 899.	1.3	2
248	Precise patterning of SiO2-based glass by low-temperature nanoimprint lithography assisted by UV irradiation on both faces using Glasia® as a precursor. Journal of Vacuum Science & Technology B, 2007, 25, 1393-1397.	1.3	4
249	Contact-metal dependent current injection in pentacene thin-film transistors. Applied Physics Letters, 2007, 91, .	1.5	137
250	Frequency response analysis of pentacene thin-film transistors with low impedance contact by interface molecular doping. Applied Physics Letters, 2007, 91, .	1.5	55
251	In-Crystal and Surface Charge Transport of Electric-Field-Induced Carriers in Organic Single-Crystal Semiconductors. Physical Review Letters, 2007, 98, 196804.	2.9	161
252	Suppression of short channel effect in organic thin film transistors. Applied Physics Letters, 2007, 91, .	1.5	53

#	Article	IF	CITATIONS
253	Charge injection process in organic field-effect transistors. Applied Physics Letters, 2007, 91, .	1.5	140
254	Molecular-packing-enhanced charge transport in organic field-effect transistors based on semiconducting porphyrin crystals. Applied Physics Letters, 2007, 91, 123501.	1.5	43
255	Quasi-Periodic Coulomb Blockade Oscillations in a Single-Wall Carbon Nanotube Bundle. Solid State Phenomena, 2007, 121-123, 537-540.	0.3	Ο
256	Scaling effect on the operation stability of short-channel organic single-crystal transistors. Applied Physics Letters, 2007, 91, 063506.	1.5	16
257	Current transport in short channel top-contact pentacene field-effect transistors investigated with the selective molecular doping technique. Applied Physics Letters, 2007, 90, 193507.	1.5	62
258	Suppression of Current Hysteresis in Carbon Nanotube Thin-Film Transistors. Japanese Journal of Applied Physics, 2007, 46, L571-L573.	0.8	9
259	Electron transport in thin graphite films: Influence of microfabrication processes. Physica E: Low-Dimensional Systems and Nanostructures, 2007, 40, 241-244.	1.3	12
260	Highly Reliable Bottom-Contact Pentacene TFTs with a Poly(p-chloroxylylene) Layer Selectively Grown on a Gate-Insulator. , 2007, , .		0
261	Direct Formation of Micro-/Nanocrystalline 2,5-Dimethyl-N,Nâ€~-dicyanoquinonediimine Complexes on SiO2/Si Substrates and Multiprobe Measurement of Conduction Properties. Journal of the American Chemical Society, 2006, 128, 700-701.	6.6	25
262	Quantum dots in carbon nanotubes. Semiconductor Science and Technology, 2006, 21, S52-S63.	1.0	41
263	10.5L: Late-News Paper: All-Organic TFT-Driven QQVGA Active-Matrix Polymer-Dispersed LCD with Solution-Processed Insulator, Electrodes, and Wires. Digest of Technical Papers SID International Symposium, 2006, 37, 123.	0.1	16
264	Magnetic Response of a Mesoscopic Superconducting Disk Surrounded by a Normal Metal. AIP Conference Proceedings, 2006, , .	0.3	0
265	Single-Electron Transistor Made from a Single Gold Colloidal Particle. AIP Conference Proceedings, 2006, , .	0.3	Ο
266	Reproducible formation of nanoscale-gap electrodes for single-molecule measurements by combination of FIB deposition and tunneling current detection. Microelectronic Engineering, 2006, 83, 1471-1473.	1.1	19
267	Nano-scale interface controls for future plastic transistors. Science and Technology of Advanced Materials, 2006, 7, 231-236.	2.8	7
268	Two-Dimensional Near-Field Optical Spectroscopy in Magnetic Fields up to 4 T. Optical Review, 2006, 13, 276-278.	1.2	1
269	Nano-size molecular conductors on silicon substrate-Toward device integration of conductive CT salts Journal of Low Temperature Physics, 2006, 142, 215-220.	0.6	10
270	Nonlinear optical polymer patterned by nanoimprint lithography as a photonic crystal waveguide structure. Journal of Vacuum Science & Technology B, 2006, 24, 271.	1.3	8

#	Article	IF	CITATIONS
271	Direct nanoimprint of inorganic-organic hybrid glass. Journal of Vacuum Science & Technology B, 2006, 24, 1402.	1.3	14
272	Copper Phthalocyanine Single-crystal Field-effect Transistors Stable Above 100°C. Materials Research Society Symposia Proceedings, 2006, 937, 1.	0.1	0
273	Hall Effect in Organic Single-crystal Field-effect Transistors. Materials Research Society Symposia Proceedings, 2006, 937, 1.	0.1	1
274	Surface Modifications using Thiol Self-Assembled Monolayers on Au Electrodes in Organic Field Effect Transistors. Materials Research Society Symposia Proceedings, 2006, 965, 1.	0.1	0
275	Contact resistance modulation in carbon nanotube devices investigated by four-probe experiments. Applied Physics Letters, 2006, 88, 053118.	1.5	18
276	Organic light-emitting diode driven by organic thin film transistor on plastic substrates. Journal of Applied Physics, 2006, 99, 064506.	1.1	27
277	Interface modification of a pentacene field-effect transistor with a submicron channel. Applied Physics Letters, 2006, 89, 113507.	1.5	39
278	High-density electrostatic carrier doping in organic single-crystal transistors with polymer gel electrolyte. Applied Physics Letters, 2006, 88, 112102.	1.5	91
279	Charge transport of copper phthalocyanine single-crystal field-effect transistors stable above 100°C. Applied Physics Letters, 2006, 88, 122110.	1.5	26
280	Gate capacitance in electrochemical transistor of single-walled carbon nanotube. Applied Physics Letters, 2006, 88, 073104.	1.5	32
281	High-performance transparent flexible transistors using carbon nanotube films. Applied Physics Letters, 2006, 88, 033511.	1.5	123
282	Suppression of the unconventional metallic behavior by gate voltage in MWNT device. Physica E: Low-Dimensional Systems and Nanostructures, 2005, 29, 698-701.	1.3	0
283	Formation mechanism of carbon nanotubes in the gas-phase synthesis from colloidal solutions of nanoparticles. Current Applied Physics, 2005, 5, 128-132.	1.1	19
284	Polarization measurements in tip-enhanced Raman spectroscopy applied to single-walled carbon nanotubes. Chemical Physics Letters, 2005, 410, 136-141.	1.2	77
285	Control of Carrier Density by a Solution Method in Carbon-Nanotube Devices. Advanced Materials, 2005, 17, 2430-2434.	11.1	89
286	Effect of probe configuration on spin accumulation in lateral spin-valve structure. Journal of Magnetism and Magnetic Materials, 2005, 286, 88-90.	1.0	16
287	Ion Emitter based on Carbon Nanotubes in Liquid Helium. Journal of Low Temperature Physics, 2005, 138, 899-903.	0.6	8
288	Suppression of bias- and temperature-dependent conductance by gate-voltage in multi-walled carbon nanotube. AIP Conference Proceedings, 2005, , .	0.3	1

#	Article	IF	CITATIONS
289	Hall Effect of Quasi-Hole Gas in Organic Single-Crystal Transistors. Japanese Journal of Applied Physics, 2005, 44, L1393-L1396.	0.8	154
290	Alignment-Free Top-Contact Formation for Organic Thin Film Transistors with Submicron-Length Channel. Japanese Journal of Applied Physics, 2005, 44, L479-L481.	0.8	7
291	Modification of the electric conduction at the pentaceneâ^•SiO2 interface by surface termination of SiO2. Applied Physics Letters, 2005, 86, 103502.	1.5	130
292	Proximity effect in a superconductor-metallofullerene-superconductor molecular junction. Physical Review B, 2005, 72, .	1.1	58
293	Current distribution insidePyâ^•Culateral spin-valve devices. Physical Review B, 2005, 71, .	1.1	36
294	Nano-scale fabrication and nano-scale interface control for molecular/organic devices. , 2005, , .		0
295	Pentacene transistor encapsulated by poly-para-xylylene behaving as gate dielectric insulator and passivation film. Applied Physics Letters, 2005, 87, 183502.	1.5	38
296	Superconductivity in Long and Short Molecules. AIP Conference Proceedings, 2004, , .	0.3	0
297	Purification of Single-Wall Carbon Nanotubes Synthesized from Alcohol by Catalytic Chemical Vapor Deposition. Japanese Journal of Applied Physics, 2004, 43, L396-L398.	0.8	25
298	Enhancement of nonlocal spin-valve signal using spin accumulation in local spin-valve configuration. Applied Physics Letters, 2004, 85, 5382-5384.	1.5	8
299	Spin-dependent boundary resistance in the lateral spin-valve structure. Applied Physics Letters, 2004, 85, 3501-3503.	1.5	82
300	Gate-induced crossover from unconventional metals to Fermi liquids in multiwalled carbon nanotubes. Applied Physics Letters, 2004, 85, 6404-6406.	1.5	7
301	Gate-Voltage Dependence of Zero-Bias Anomalies in Multiwall Carbon Nanotubes. Physical Review Letters, 2004, 92, 036801.	2.9	65
302	Suppression of spin accumulation in nonmagnet due to ferromagnetic ohmic contact. Applied Physics Letters, 2004, 85, 3795-3796.	1.5	35
303	Domain wall drag due to dc current injection into ferromagnetic nano-wires. Journal of Magnetism and Magnetic Materials, 2004, 272-276, E1347-E1348.	1.0	1
304	Growth control of pentacene films on SiO2/Si substrates towards formation of flat conduction layers. Thin Solid Films, 2004, 467, 168-171.	0.8	18
305	Non-local Hall resistance measured in submicron-scale non-magnetic/ferromagnetic junctions. Journal of Magnetism and Magnetic Materials, 2004, 272-276, E1333-E1334.	1.0	9
306	Direct observation of contact and channel resistance in pentacene four-terminal thin-film transistor patterned by laser ablation method. Applied Physics Letters, 2004, 84, 813-815.	1.5	105

#	Article	IF	CITATIONS
307	Pentacene nanotransistor with carbon nanotube electrodes. Applied Physics Letters, 2004, 85, 1021-1023.	1.5	44
308	Fabrication of Coulomb blockade device utilizing the 0.34 nm interlayer spacing in a multiwalled carbon nanotube. Microelectronic Engineering, 2004, 73-74, 666-669.	1.1	2
309	Carbon nanotubes with a nanogap for nanoscale organic devices. Microelectronic Engineering, 2004, 73-74, 675-678.	1.1	13
310	The formation of nanometer-scale gaps by electrical degradation and their application to C60 transport measurements. Microelectronic Engineering, 2004, 73-74, 686-688.	1.1	12
311	Multiple-layer conduction and scattering property in multi-walled carbon nanotubes. New Journal of Physics, 2004, 6, 3-3.	1.2	9
312	High-yield production of single-wall carbon nanotubes in nitrogen gas. Chemical Physics Letters, 2003, 372, 45-50.	1.2	54
313	Catalytic growth of carbon nanotubes and their patterning based on ink-jet and lithographic techniques. Journal of Electroanalytical Chemistry, 2003, 559, 25-30.	1.9	27
314	Temperature-mediated switching of magnetoresistance in Co-contacted multiwall carbon nanotubes. Applied Physics Letters, 2003, 83, 1008-1010.	1.5	20
315	Coulomb blockade oscillation in a multiwalled carbon nanotube with internanotube tunnel junctions. Applied Physics Letters, 2003, 83, 1429-1431.	1.5	10
316	Suppressed pinning field of a trapped domain wall due to direct current injection. Journal of Applied Physics, 2003, 94, 7266-7269.	1.1	25
317	Spin-current-assisted domain-wall depinning in a submicron magnetic wire. Journal of Applied Physics, 2003, 94, 7947.	1.1	26
318	High density current operation in nanographite fiber synthesized by chemical vapor deposition. Journal of Applied Physics, 2003, 94, 3516-3519.	1.1	3
319	One-dimensional System in Carbon Nanotubes. AIP Conference Proceedings, 2003, , .	0.3	5
320	A Reliable Method for Fabricating sub-10 nm Gap Junctions Without Using Electron Beam Lithography. E-Journal of Surface Science and Nanotechnology, 2003, 1, 41-44.	0.1	46
321	Carbon Nanotubes for Nanoscale Spin-Electronics. , 2003, , 433-456.		1
322	Charge transfer control by gate voltage in crossed nanotube junction. Applied Physics Letters, 2002, 81, 2250-2252.	1.5	16
323	Magnetic field dependence of Coulomb oscillations in metal/multi-wall carbon nanotube/metal structures. Physica B: Condensed Matter, 2002, 323, 246-248.	1.3	10
324	Carbon nanotube devices for nanoelectronics. Physica B: Condensed Matter, 2002, 323, 107-114.	1.3	138

#	Article	IF	CITATIONS
325	Resistance dependence of transport properties in metal–multiwall carbon nanotube–metal structures. Microelectronic Engineering, 2002, 63, 33-37.	1.1	4
326	Spin transport in nanotubes (invited). Journal of Applied Physics, 2001, 89, 6863-6867.	1.1	39
327	Observation of Coulomb blockade in a Ti/multi-wall carbon nanotube/Ti structure. AIP Conference Proceedings, 2001, , .	0.3	0
328	Spin transport in nanotubes. Materials Science and Engineering B: Solid-State Materials for Advanced Technology, 2001, 84, 26-30.	1.7	10
329	Magnetoresistance of ferromagnetically contacted carbon nanotubes. Physica E: Low-Dimensional Systems and Nanostructures, 2001, 10, 499-504.	1.3	10
330	Nanoscale Coulomb blockade memory and logic devices. Nanotechnology, 2001, 12, 155-159.	1.3	20
331	Electron transport in metal/multiwall carbon nanotube/metal structures (metal=Ti or Pt/Au). Applied Physics Letters, 2001, 79, 1354-1356.	1.5	45
332	Coulomb blockade in multiwalled carbon nanotube island with nanotube leads. Applied Physics Letters, 2001, 79, 1465-1467.	1.5	28
333	Nano-Device Formation in a Multi-Wall Carbon Nanotube. , 2001, , .		0
334	Quantum-dot transport in carbon nanotubes. Superlattices and Microstructures, 2000, 27, 551-554.	1.4	8
335	Spin-polarized transport in carbon nanotubes. Superlattices and Microstructures, 2000, 27, 565-570.	1.4	12
336	Spin electronics using carbon nanotubes. Physica E: Low-Dimensional Systems and Nanostructures, 2000, 6, 848-851.	1.3	21
337	Scaling of the single-electron tunnelling current through ultrasmall tunnel junctions. Journal of Physics Condensed Matter, 2000, 12, 7223-7228.	0.7	0
338	Coherent transport of electron spin in a ferromagnetically contacted carbon nanotube. Nature, 1999, 401, 572-574.	13.7	743
339	Current Hysteresis in a Delta Doped GaAs Metal-Semiconductor Field Effect Transistor. , 1999, , .		0
340	Commensurability oscillations by runaway and pinned electrons. Superlattices and Microstructures, 1998, 23, 493-497.	1.4	7
341	Two-way switching based on turnstile operation. Applied Physics Letters, 1998, 72, 1084-1085.	1.5	14
342	Operation of logic function in a Coulomb blockade device. Applied Physics Letters, 1998, 73, 2515-2517.	1.5	32

#	Article	IF	CITATIONS
343	Detection of Spin-Flip Relaxation Using Quantum Point Contacts. Physical Review Letters, 1998, 81, 5628-5631.	2.9	6
344	Electron pump in multiple-tunnel junctions. Physical Review B, 1997, 56, 3972-3975.	1.1	17
345	Electron pump current by two pulses with phase delay. Applied Physics Letters, 1997, 71, 3138-3140.	1.5	11
346	Turnstile Based Single-Electron Logic Devices. , 1997, , .		0
347	Investigation of Hall Resistivity in Antidot Lattices with respect to Commensurability Oscillations. Journal of the Physical Society of Japan, 1996, 65, 1914-1916.	0.7	11
348	On the Mechanism of Commensurability Oscillations in Anisotropic Antidot Lattices. Journal of the Physical Society of Japan, 1996, 65, 811-817.	0.7	24
349	Mechanism of commensurability oscillations in anisotropic antidot lattice. Physica B: Condensed Matter, 1996, 227, 141-143.	1.3	1
350	Magnetotransport through disordered and anisotropic antidot lattices in GaAs/AlxGa1â^'xAs heterostructures. Physical Review B, 1995, 52, 8344-8347.	1.1	46
351	Current-Direction-Dependent Commensurate Oscillations in GaAs/AlGaAs Antidot Superlattice. Japanese Journal of Applied Physics, 1995, 34, 4335-4337.	0.8	17
352	Magnetic Electron Focusing Effect in GaAs/AlGaAs Heterostructure with Gate-Controlled Byway Channel. Japanese Journal of Applied Physics, 1995, 34, 4329-4331.	0.8	0
353	Mechanism of apparent reflection of electrons from extra probes investigated by the magnetic electron-focusing effect. Physical Review B, 1994, 50, 11661-11665.	1.1	2
354	Transport properties in artificial lateral superlattice. Superlattices and Microstructures, 1994, 16, 295-301.	1.4	15
355	Angular distribution of emitted electrons from wire by magnetic electron focusing effect and low field magnetoresistance. Solid State Communications, 1994, 92, 413-417.	0.9	2
356	Influence of gate voltage on nonlocal resistance in GaAs/ AlGaAs heterostructure at high magnetic fields. Physica B: Condensed Matter, 1993, 184, 21-25.	1.3	3
357	Investigation of ballistic elastic scattering length and specularity in multiterminal GaAs/AlGaAs by magnetic electron focusing effect. Applied Physics Letters, 1993, 62, 1609-1611.	1.5	15
358	Role of edge and bulk currents through a gate barrier in nonlocal resistance of GaAs/AlxGa1â^'xAs. Physical Review B, 1992, 46, 5016-5019.	1.1	8
359	Nonlocal quantum conduction and the influence of contact resistance in GaAs/AlGaAs wires. Surface Science, 1992, 267, 282-285.	0.8	14
360	Ballistic and elastic mean free paths determined by magnetic electron focusing effect in GaAs/AlGaAs. Solid State Communications, 1992, 83, 775-777.	0.9	5

#	Article	IF	CITATIONS
361	Spin-Dependent Nonlocal Quantum Transport Influenced by Gate Voltage in GaAs/AlGaAs Wires. , 1992, , 199-204.		0
362	Influence of edge current and contact on nonlocal Shubnikov-de Haas oscillations in macroscopic GaAs/AlGaAs wire. Solid State Communications, 1991, 80, 571-574.	0.9	18
363	Nonlocal Shubnikov-de Haas oscillations through edge and bulk currents in GaAs/AlGaAs mesoscopic quantum wires. Solid State Communications, 1991, 80, 797-800.	0.9	13
364	A search for multiplicity fluctuations in high energy nucleus-nucleus collisions. Physics Letters, Section B: Nuclear, Elementary Particle and High-Energy Physics, 1990, 252, 303-310.	1.5	35
365	An emulsion study of 16O and 32S interactions at 200 GeV per nucleon selected by transverse energy. Nuclear Physics B, 1990, 342, 279-301.	0.9	11
366	The production of charmed particles in high-energy 16O-emulsion central interactions. Physics Letters, Section B: Nuclear, Elementary Particle and High-Energy Physics, 1989, 224, 441-444.	1.5	11
367	Spin injection in carbon nanotubes. , 0, , .		0
368	Nanostructure construction in single-walled carbon nanotubes by AFM manipulation. , 0, , .		13
369	Nano-electronics in a multiwall carbon nanotube. , 0, , .		1
370	Inter-Layer Screening Length to Electric Field in Thin Graphite Film. Applied Physics Express, 0, 1, 034007.	1.1	78
371	Coulomb Blockade Oscillations in Narrow Corrugated Graphite Ribbons. Applied Physics Express, 0, 1, 024001.	1.1	15
372	Performance Enhancement of Thin-Film Transistors by Using High-Purity Semiconducting Single-Wall Carbon Nanotubes. Applied Physics Express, 0, 2, 071601.	1.1	33
373	Ambipolar to Unipolar Irreversible Switching in Nanosheet Transistors: The Role of Ferrocene in Fullerene/Ferrocene Nanosheets. Journal of Materials Chemistry C, 0, , .	2.7	5